Local structure and dynamics of a segregated $c(2\times2)$ sulfur layer on Pd(001) studied by scanning tunneling microscopy

D. Bürgler, G. Tarrach, T. Schaub, R. Wiesendanger, and H.-J. Güntherodt
Institut für Physik, Universität Basel, Klingelbergstrasse 82, CH-4056 Basel, Switzerland
(Received 16 November 1992)

We report a scanning-tunneling-microscopy study of a S overlayer on Pd(001) obtained by diffusion of S atoms from the bulk to the surface. Atomically resolved images display the $c(2\times2)$ symmetry of the saturation coverage. A large variety of defects such as steps, vacancies, and antiphase domain boundaries were imaged. The high density of domain boundaries reduces the effective coverage to only 0.4 monolayer and stabilizes this nonideal overlayer. A model of the growth mechanism is proposed. Changes of the atomic structure on a time scale of a few minutes were observed and are discussed.

A saturated S overlayer on Pd(001) was first investigated by Berndt, Hora, and Scheffler[1] using intensity analysis of low-energy-electron-diffraction (LEED) patterns. It was found that the S atoms adsorb in fourfold-hollow positions yielding a $c(2\times2)$ symmetry. Several authors used the S/Pd(001) system to study the poisoning effect of S on adsorption, desorption and reactions of NO,[2] SO_2,[3] and CO.[4] The chemistry of these gases on transition-metal surfaces is of interest, since it plays a crucial role in catalysis. Surface defects are known as sites of enhanced reactivity and nucleation probability for many processes. Therefore, the detailed knowledge of their distribution and atomic structure is of great importance. Scanning tunneling microscopy (STM) is an ideal tool to gain this information, which is hardly accessible by diffraction techniques (e.g., LEED) due to the lack of periodicity. STM studies of S overlayers on Pd(111),[5] Pt(001),[6] Mo(001),[7] Re(0001),[8] and copper[9] have recently been reported and revealed very different atomic structures.

The present study was performed in a four-chamber ultrahigh-vacuum (UHV) system (base pressure below 10^{-10} mbar) equipped with ion guns and heating stages for sample preparation and with standard surface-analysis facilities, such as Auger electron and x-ray photoelectron spectroscopy (AES and XPS) for sample characterization. The scanning tunneling microscope is described in detail elsewhere.[10,11]

The mechanically polished (001) surface of the Pd single crystal was prepared by cycles of Ar^+-ion etching and subsequent annealing to a maximum temperature of 1070±50 K. The heating was done by electron bombardment from the rear side to avoid structural damage. A dual-wavelength pyrometer was used to measure the specimen's surface temperature. After each step of preparation, the chemical composition of the sample surface was monitored by XPS and AES. Figure 1 shows a comparison of the Auger spectra obtained after ion etching (1-keV Ar^+ ions, 0.8 $\mu A/cm^2$ for 10 min) in the lower curve and after subsequent annealing (upper curve). Whereas the Pd peaks are identical in the two spectra, the upper curve displays an additional peak at 152 eV corresponding to the LMM Auger transition of sulfur. Horn *et al.*[12] have shown that an ordered S overlayer on Pd(001) can be obtained by diffusion of S atoms from the bulk to the surface at about 1000 K. Note that oxygen (main peak at 503 eV) is not detectable in either spectrum. It is difficult to estimate the amount of C contamination from AES, because the C peak at 272 eV overlaps the Pd peak at 279 eV. However, XPS measurements reveal only minor traces of C on the surface.

All STM images in this paper were acquired at room temperature in the constant-current mode using chemically etched W tips. Figure 2 demonstrates atomic resolution that could be obtained routinely with positive and negative sample biases (U) in the range from 200 to 630 mV and tunnel currents (I) between 80 pA and 1 nA. In agreement with calculations by Feibelman and Hamann[13] and Lang,[14] we identify the bright spots as chemisorbed S atoms. The measured lattice constant of 0.39±0.04 nm within ordered regions agrees well with the 0.389-nm periodicity of $c(2\times2)$-ordered adatoms on a Pd(001) surface. We determined a corrugation of 0.01 nm within ordered regions and 0.03 nm across boundaries. These values did not depend on the tunneling parameters.

The dark lines between ordered regions represent antiphase domain boundaries separating the two equivalent domain types of the $c(2\times2)$ reconstruction. Figure 3

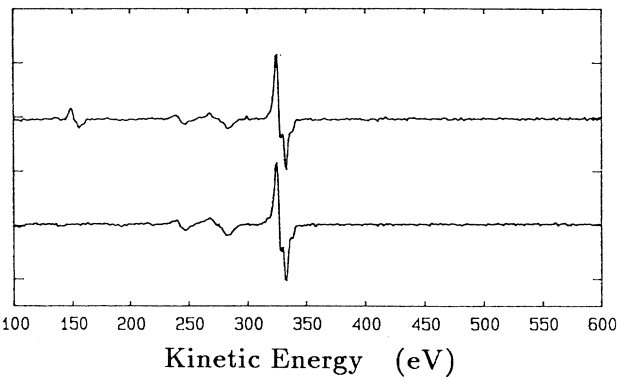

FIG. 1. Differentiated AES spectra of the Pd(001) surface immediately after ion etching (lower curve) and subsequent annealing to 1070 K (upper curve). In the spectrum of the annealed surface, an additional peak appears at 152 eV due to the S overlayer.

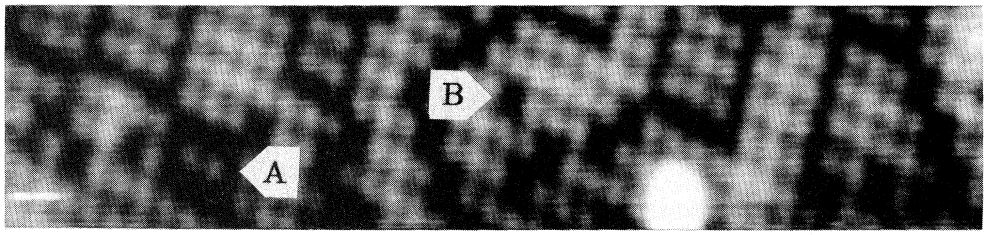

FIG. 2. Topographic STM image ($I=0.5$ nA, $U=+630$ mV) of a 15.7×3.8 nm^2 large, flat region showing the atomic structure of the S overlayer after the first annealing cycle. Label *A* marks a "two-atom domain" and *B* a vacancy-type defect.

shows a sketch of such boundaries. The domains in the right-hand part are separated by a kinked boundary. Note that the lower left and upper right domain have the same phase and touch each other at the corners. The STM images do not show any preferred shape of the domains, and the number of atoms per domain also varies strongly. There are domains consisting of only two atoms (label *A* in Fig. 2) or even one (label *A* in Fig. 4). The atomic structure of a "single-atom domain" is depicted in the lower-left part of Fig. 3. The four steps imaged in Fig. 4 are 0.20 ± 0.01 nm high and correspond to monatomic steps of the Pd substrate of 0.195-nm height. The dark isolated dots that fit the registry of the S adatoms (label *B* in Fig. 2) are places where a single S atom is missing. Such a vacancy-type defect is modeled in the upper-right corner of Fig. 3.

Counting the adatoms present on the imaged surface areas allows us to accurately determine the effective S coverage (σ_{eff}). The value obtained from images taken after annealing the sample at 1070 ± 50 K for 19 h is $\sigma_{\text{eff}}=0.39\pm0.01$ monolayer (ML) with respect to the Pd bulk termination. After further annealing for 9 h at the same temperature σ_{eff} was 0.40 ± 0.02 ML.

Figure 5 shows two images of the same region on the surface, with (b) taken 4 min after (a) using the same tunneling parameters. The inspection of such comparative images reveals changes in the atomic arrangement on this time scale, where 3–4 % of the atoms appear on new positions. Each change affects a small number of atoms,

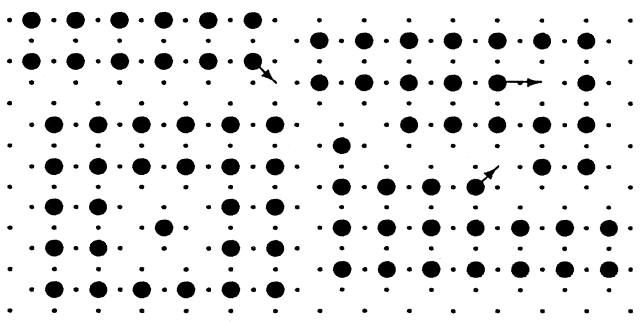

FIG. 3. Schematic picture of the $c(2\times2)$ reconstruction. Small dots are Pd atoms and large dots represent S adatoms sitting on the hollow sites of the Pd lattice. Straight and kinked antiphase domain boundaries, a vacancy-type defect (upper right) and a "single-atom domain" (lower left) are modeled. The arrows indicate possible single-atom rearrangements.

often only one, and can be considered as a series of single-atom motions. In principle, an atom can hop within a domain to a vacancy site, or move at the border of domains either at corners or kink sites. These possibilities are indicated in Fig. 3 by three arrows. Interestingly, all observed changes took place at domain boundaries (see arrows in Fig. 5). Note that the bright spot labeled *A* in Fig. 5(a) has gone in Fig. 5(b) and a perfect domain is visible instead. The nature of the bright spots is not known. Possibly, they are C contaminations or S clusters sitting on top of the ordered overlayer.

Based on our results, we propose the following model for the formation of the S overlayer on Pd(001): S atoms diffusing randomly through the bulk at elevated temperatures reach the surface and are chemisorbed at hollow sites.[1] Their surface mobility is highly reduced due to the strong S-Pd interaction. The presence of an adatom blocks chemisorption on the four neighboring hollow sites at a distance of 0.275 nm, which is much smaller than the van der Waals diameter of S (0.36 nm). Locally, this leads to the formation of the $c(2\times2)$ reconstruction, which is the saturation coverage of S on Pd(001) (Ref. 2) corresponding to 0.5 ML of S. The existence of two phase-shifted, equivalent domain types gives rise to the formation of antiphase domain boundaries, when the coverage reaches saturation. Vacancy-type defects persist during the growth, because the probability of hitting such a site decreases with their number. When the overlayer is saturated, the incorporation of an additional S atom is still possible at vacancy-type defects and unlikely at all other sites, because at least one atom has to move to a neighboring hollow site.

The same qualitative appearance and the equal effective coverage before and after additional annealing (see Figs. 2 and 4) demonstrate the lack of an efficient relaxation mechanism of the overlayer which would allow a reduction in the number of defects and an increase in coverage. A slightly smaller density of vacancy-type defects in the images acquired after additional annealing supports our model.

We now discuss the dynamics of a saturated overlayer at room temperature. The atomic rearrangements presented in Fig. 5 suggest that there is a probability for an adatom hopping across a bridge site to an unoccupied and unblocked hollow site. These sites are only available at corners and kinks of antiphase domain boundaries (see short arrows in Fig. 3). A series of such single-atom motions can cause a domain boundary movement, as seen in the top left corner of Fig. 5. We have never observed

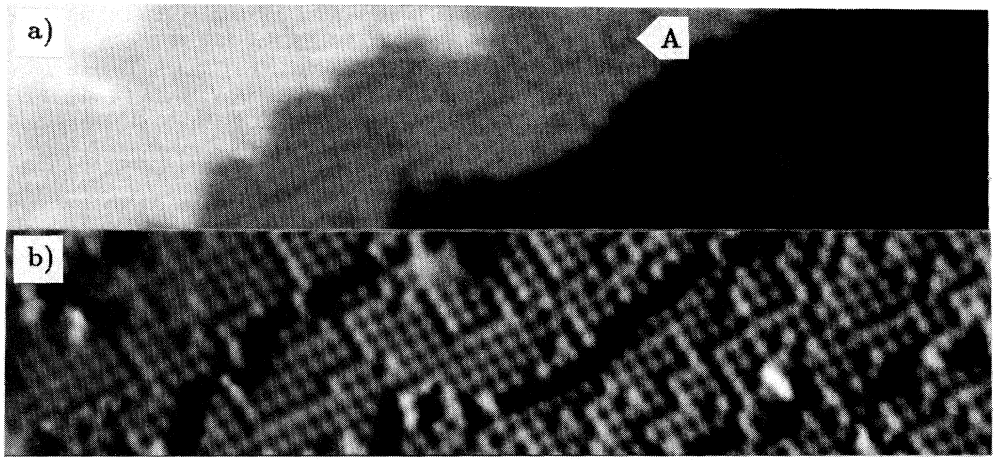

FIG. 4. STM image ($I = 0.5$ nA, $U = +630$ mV) of a stepped region acquired after an additional annealing cycle: grey-scale (a) and derivative (b) representation. The area shown is 21.8×5.3 nm^2. The atomic structure looks qualitatively the same as in Fig. 2. Label A marks a "single-atom domain."

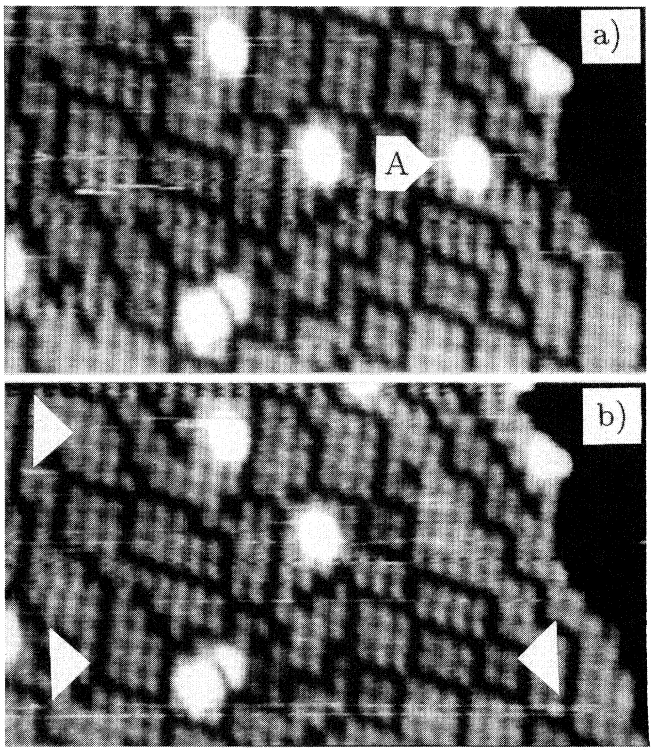

FIG. 5. Two STM images ($I = 1$ nA, $U = +630$ mV) showing the same area of the surface imaged successively: (b) was imaged 4 min after (a). The arrows indicate spots where the atomic arrangement has changed. The areas shown are 13.6×8.3 nm^2.

the hopping of an atom across a top site to a vacancy site (see the long arrow in Fig. 3). Therefore, we conclude that the potential barrier at a top site is much higher than at a bridge site. This is in agreement with the general trend of S to chemisorb on metal surfaces at sites with the highest available coordination number. The electronegativity of S leads to a strong repulsive adatom-adatom interaction which must have short-range character, since any long-range interaction would tend to induce an ordered domain structure on this length scale. This is clearly not the case in our images.

Possibly, the thermal energy at room temperature is not sufficient to activate single-atom motions on the free surface, and the observed changes are induced by the close proximity of the STM tip to the surface. The strong electric field at the tip apex and the forces acting on the surface atoms originating from tip-surface interactions[15] might be mechanisms for the activation of single-atom motions.

In conclusion, we have presented STM images of the atomic arrangement of a S overlayer on a Pd(001) surface. The observed structures with small domains separated by antiphase boundaries, and the resulting reduced effective coverage are explained by a model for the growth mechanism. This model combines random diffusion of the S atoms to the surface with a highly reduced surface mobility. Local dynamics at room temperature are based upon single-atom motions over bridge sites. They may occur if an unoccupied and unblocked neighboring hollow site is available.

Financial support from the Swiss National Science Foundation and the Kommission zur Förderung der wissenschaftlichen Forschung is gratefully acknowledged.

[1]W. Berndt, R. Hora, and M. Scheffler, Surf. Sci. **117**, 188 (1982).
[2]S. W. Jorgensen, N. D. S. Canning, and R. J. Madix, Surf. Sci. **179**, 322 (1987).
[3]M. L. Burke and R. J. Madix, Surf. Sci. **194**, 223 (1988).
[4]S. W. Jorgensen and R. J. Madix, Surf. Sci. **163**, 19 (1985).
[5]A. J. Gellman, J. C. Dunphy, and M. Salmeron, Langmuir **8**, 534 (1992).
[6]V. Maurice and P. Marcus, Surf. Sci. **262**, L59 (1992).
[7]B. Marchon, P. Bernhardt, M. E. Bussell, G. A. Somorjai, M. Salmeron, and W. Siekhaus, Phys. Rev. Lett. **60**, 1166 (1988).
[8]D. F. Ogletree, R. Q. Hwang, D. M. Zeglinski, A. Lopez Vazquez de Parga, G. A. Somorjai, and M. Salmeron, J. Vac. Sci. Technol. B **9**, 886 (1991).
[9]I. Steensgaard, L. Ruan, F. Besenbacher, F. Jensen, and E. Lægsgaard, Surf. Sci. **269**, 81 (1992).
[10]R. Wiesendanger, G. Tarrach, D. Bürgler, T. Jung, L. Eng, and H.-J. Güntherodt, Vacuum **41**, 386 (1990).
[11]R. Wiesendanger, D. Bürgler, G. Tarrach, D. Anselmetti, H. R. Hidber, and H.-J. Güntherodt, J. Vac. Sci. Technol. A **8**, 339 (1990).
[12]K. Horn, N. V. Richardson, A. M. Bradshaw, and J. K. Sass, Solid State Commun. **32**, 161 (1979).
[13]P. J. Feibelman and D. R. Hamann, Surf. Sci. **149**, 48 (1985).
[14]N. D. Lang, Phys. Rev. Lett. **56**, 1164 (1986).
[15]M. Salmeron, D. F. Ogletree, C. Ocal, H.-C. Wang, G. Neubauer, W. Kolbe, and G. Meyers, J. Vac. Sci. Technol. B **9**, 1347 (1991).

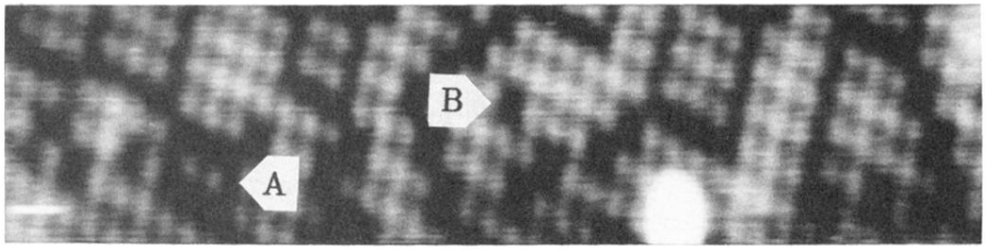

FIG. 2. Topographic STM image ($I = 0.5$ nA, $U = +630$ mV) of a 15.7×3.8 nm^2 large, flat region showing the atomic structure of the S overlayer after the first annealing cycle. Label *A* marks a "two-atom domain" and *B* a vacancy-type defect.

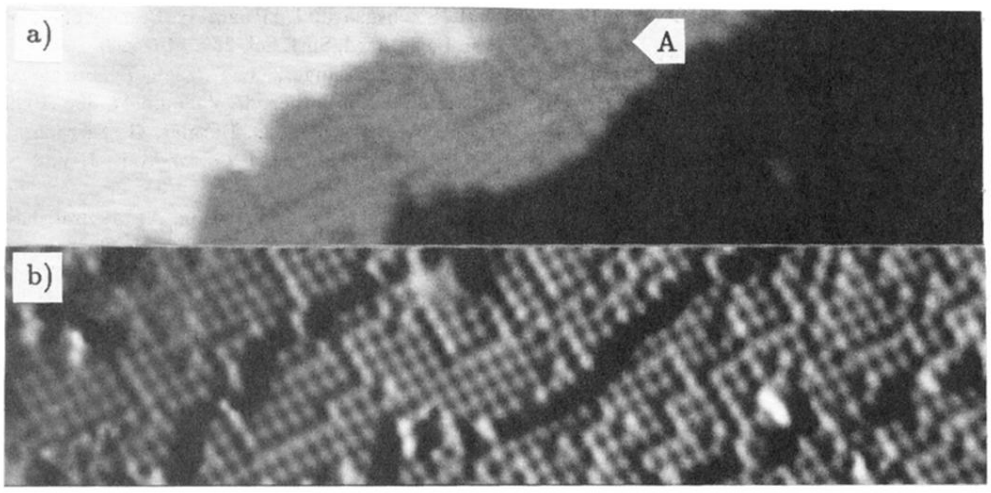

FIG. 4. STM image ($I = 0.5$ nA, $U = +630$ mV) of a stepped region acquired after an additional annealing cycle: grey-scale (a) and derivative (b) representation. The area shown is 21.8×5.3 nm^2. The atomic structure looks qualitatively the same as in Fig. 2. Label *A* marks a "single-atom domain."

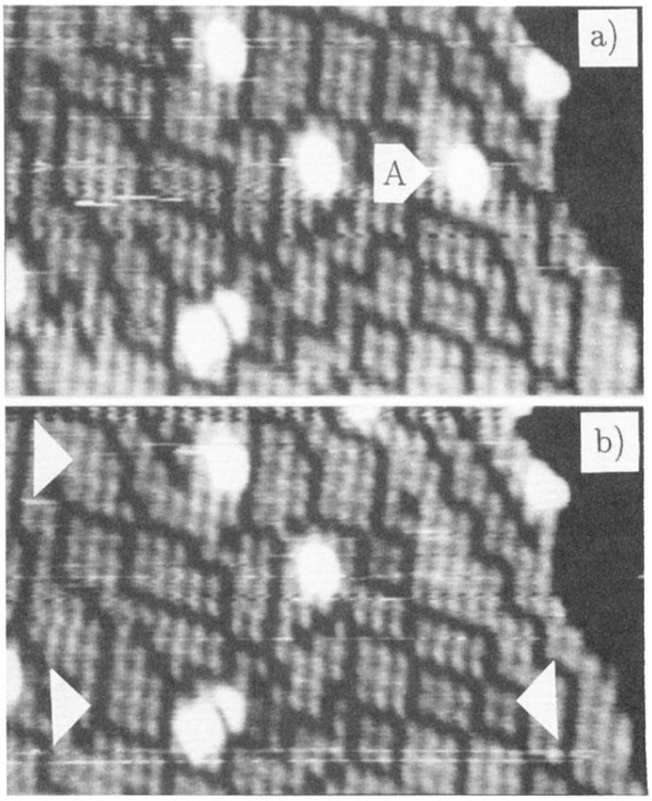

FIG. 5. Two STM images ($I = 1$ nA, $U = +630$ mV) showing the same area of the surface imaged successively: (b) was imaged 4 min after (a). The arrows indicate spots where the atomic arrangement has changed. The areas shown are 13.6×8.3 nm^2.